Imaging Evaluation of the Painful or Failed Shoulder Arthroplasty

19

Lawrence V. Gulotta and Gabrielle Konin

19.1 Background

Shoulder arthroplasty has led to successful results in over 90% of cases with an estimated complication rate of about 15% [1–5]. Not all complications, however, lead to undesirable outcomes for the patient. Conversely, the absence of complications does not ensure a good clinical result, such as with stiffness or unexplained pain [6]. For this reason, shoulder arthroplasty failure is a broader term that also encompasses patient dissatisfaction with the result of the procedure, regardless of the severity of symptoms or physical findings [7]. Using this definition, Hasan and colleagues studied 144 shoulder arthroplasties and observed the following characteristics of failure in descending order: stiffness, instability, rotator cuff tear, nonunion of the tuberosities or surgical neck, glenoid component loosening, glenoid erosion, glenoid polyethylene wear, component malposition, humeral component loosening, periprosthetic fracture, infection, nerve injury, and heterotopic bone [6].

Similar to the findings by Hasan et al. [6], other investigators have identified common trends in complications after shoulder arthroplasty, although the complication rate varies depending on the study. In another study, Cofield [4] reported a 14% complication rate and identified eight major causes in decreasing frequency: instability, rotator cuff tear, heterotopic ossification, glenoid component loosening, intraoperative fracture, nerve injury, infection, and humeral component loosening. More recently, Bohsali and colleagues [8] performed a large retrospective review of 39 studies involving 2810 TSA and reported a 14.7% complication rate. The most common complications, in order of frequency, were component loosening, instability, periprosthetic fracture, rotator cuff tears, neural injury, infection, and deltoid muscle dysfunction.

The imaging evaluation of the painful or failed shoulder arthroplasty should be used in conjunction with a careful history and physical examination and directed laboratory testing, if indicated. Plain radiographs provide substantial information about bone and soft tissue pathology and thus comprise the initial imaging modality to evaluate a shoulder arthroplasty. At least two mutually orthogonal images should be obtained. The glenohumeral anteroposterior (AP) and axillary lateral projections fulfill this requirement [9].

Unlike hip and knee arthroplasty, there is no established comprehensive protocol for evaluating the optimal position of a shoulder implant. Authors have made general recommendations based on observations. Iannotti et al. [10] suggest the humeral component should sit above the level of the tuberosity by less than 1 cm to avoid impingement and rotator cuff tears. Figgie et al. [11] found that functional outcome correlated with the position of the glenoid and humeral components. When the height of the humeral head above the tuberosity and the glenoid and humeral offsets were restored, there was an improved range of motion and reduced incidence of lucent lines compared with patients without restoration of correct alignment. Long-term vigilance is required when caring for shoulder arthroplasty patients because complications often present in a delayed fashion. Deshmukh et al. [12] analyzed complications with respect to the time of occurrence and found that, on the average, component loosening was found at 7.7 ± 4.8 years; infections, at 12.1 ± 2.9 years; dislocations, at 2.1 ± 3.6 years; and periprosthetic fractures, at 5.8 ± 4.7 years. No matter when a patient presents with complaints, a thorough knowledge of the pathological appearance on imaging is essential for quality care.

In this chapter, we will discuss some of the more common causes of TSA failure and the utility of MRI in the diagnosis and management of them. When possible, case vignettes are used to demonstrate the correlation between MRI results and the findings during revision surgery.

L. V. Gulotta (✉)
Shoulder and Elbow Division of the Sports Medicine Institute, Hospital for Special Surgery, New York, NY, USA
e-mail: gulottal@hss.edu

G. Konin
Department of Radiology and Imaging, Hospital for Special Surgery, New York, NY, USA

B. C. Werner (ed.), *MRI-Arthroscopy Correlations*, https://doi.org/10.1007/978-3-030-94789-7_19

19.2 Component Loosening

19.2.1 Case 1

A 67-year-old right-hand-dominant man who underwent a left total shoulder replacement approximately 5 years prior to presentation. He now complains of pain with range of motion. His physical exam shows forward flexion to 160°, external rotation of 45°, and internal rotation to the lumbar spine. He demonstrates excellent strength with rotator cuff testing including a negative belly press. Radiographs show some radiolucency around the glenoid component but without frank loosening (Fig. 19.1). MRI shows evidence of loosening around glenoid component (Fig. 19.2a, b).

Patient then underwent arthroscopic removal of a loose glenoid component (Fig. 19.3a–c). The component was removed through the rotator interval. At the time of arthroscopy, biopsies were taken for culture and were held for 14 days in order to rule out an indolent infection with *P. acnes*. These were negative. The patient went on to pain-free range of motion and elected not to undergo another procedure for glenoid reimplantation.

In the analysis by Bohsali et al. [8], loosening of the glenoid and humeral components occurred frequently, accounting for 39% of complications. Moreover, 83% of the cases of loosening involved failure of the glenoid component fixation. Loosening of an arthroplasty component is recognized on radiographs as the appearance of a radiolucent line at the implant/cement/bone interface. Line thickness is measured starting with 0.5 mm. Franklin et al. [13] devised criteria to classify radiolucency around the glenoid component for keeled implants (Table 19.1). Similarly, Lazarus et al. [14] developed a classification for pegged implants. However,

Fig. 19.1 Glenoid component loosening with radiolucent lines

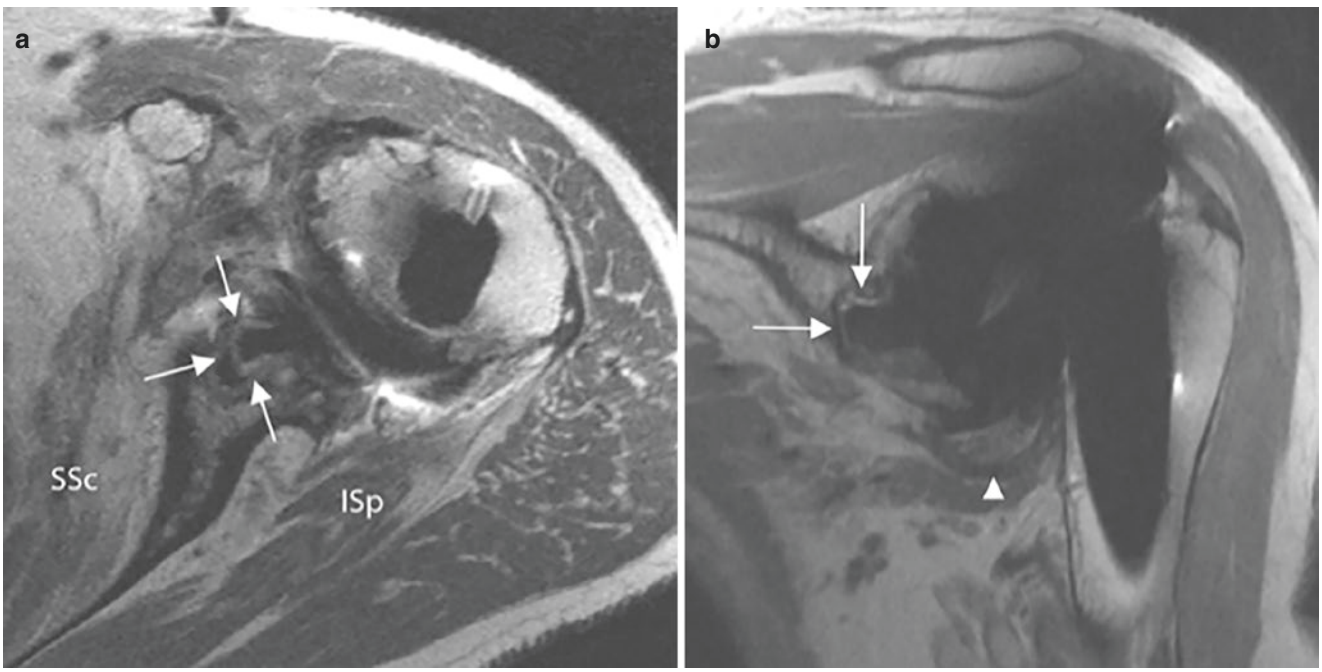

Fig. 19.2 Axial (**a**) and coronal oblique (**b**) FSE PD images demonstrate circumferential hyperintense signal with adjacent thin low-signal rim about the glenoid baseplate and keel indicative of loosening (*arrows*) in two different patients. Wear-induced synovitis is detected on the coronal oblique image at the axillary recess (*arrowhead*)

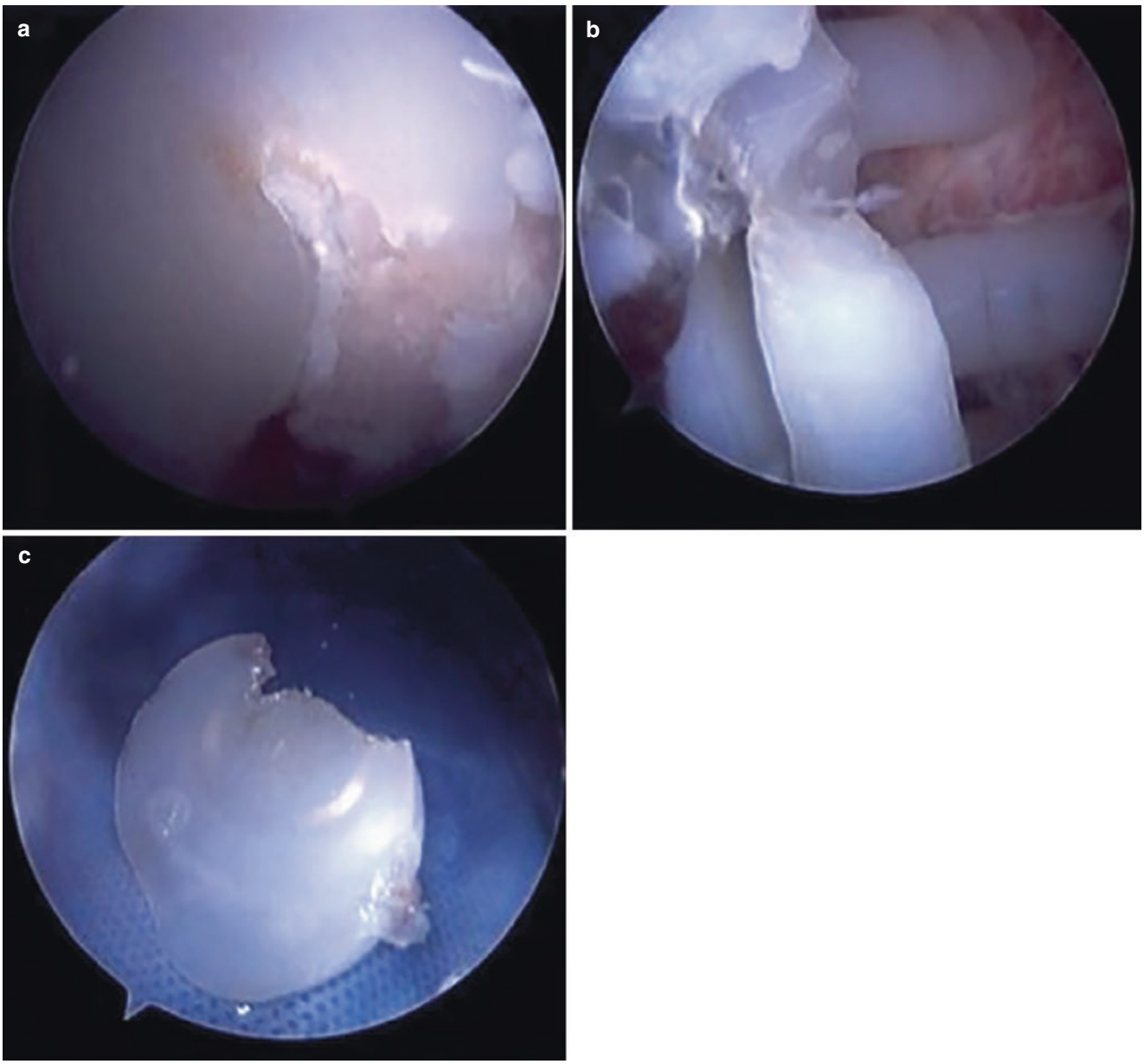

Fig. 19.3 (**a**) Arthroscopic images while viewing from a posterior portal of a cracked and loose glenoid. (**b**) Glenoid was easily removed arthroscopically through an incision made in the rotator interval. (**c**) View of the glenoid on the back table after removal

Table 19.1 Classification of radiolucency around keeled glenoid components

Grade 0	No radiolucency
Grade 1	Radiolucency at superior and/or inferior flange
Grade 2	Incomplete radiolucency at keel
Grade 3	Complete radiolucency (≤2 mm wide) around keel
Grade 4	Complete radiolucency (>2 mm wide) around keel
Grade 5	Gross loosening

From Franklin et al. [13]; with permission

relying solely on plain radiographs to determine security of fixation of the glenoid may be problematic because obtaining reproducible X-rays of the glenoid can be difficult [15]. Therefore, there is the potential that MRI may improve the accuracy of making this diagnosis.

In reverse total shoulder arthroplasty, scapular notching is another glenoid complication that can lead to implant failure. This term describes a common complication involving the erosion of the inferior scapular neck related to impingement by the medial rim of the humeral cup during adduction [16–20]. A large multicenter trial found an incidence of 68% at a mean follow-up of 51 months. It was also shown that notching was accompanied by decreases in strength and anterior elevation as well as an increased incidence in humeral and glenoid radiolucent lines [21]. Nyffeler et al. [22] concluded inferior placement of the baseplate on the glenoid plate to

prevent the occurrence of notching and also improve range of motion. Glenospheres with a lateral center of rotation have been shown to produce lower rates of scapular notching [23–25]. However, the role of MRI and arthroscopy is limited in the diagnosis and management of scapular notching following reverse shoulder arthroplasty.

With regard to the prosthetic humeral head, analyzing its position relative to the greater tuberosity and the shift of the stem in the frontal plane can identify a humeral component at risk or not at risk of loosening [26]. For additional precision in measuring shift of the stem, authors have devised various terminologies. Subsidence (S) describes the change in the vertical distance between the most superior aspects of the humeral component and the greater tuberosity [27]. The tilt is the medial or lateral change in the components' position measured by calculating the distance of the external surface of the humeral component from the external surface of cortical bone in four areas: superolateral (at the border between radiographic zones 1 and 2), inferolateral (zones 2 and 3), superomedial (zones 6 and 7), and inferomedial (zones 5 and 6) [27, 28]. Clinically relevant threshold amounts for subsidence and tilt in humeral component position are ≥5 mm and ≥10 mm, respectively [26]. Given the relative rarity of implant loosening following shoulder arthroplasty, it is imperative for the surgeon to work up and rule out infection, particularly in the setting of isolated humeral loosening.

Table 19.2 Classification of prosthetic head subluxation

Absent	The humeral head is centered in the glenoid cavity
Slight	<25% translation of the center of the head component with respect to the glenoid center
Moderate	25–50% translation of the center of the prosthetic head with respect to the glenoid center
Severe	>50% translation of the center of the head component with respect to the glenoid center

From Sperling et al. [35]; with permission

Fig. 19.4 Ultrasound image depicts an intact subscapularis tendon (*arrows*) in the long axis. *LT* lesser tuberosity, *L* lateral, *M* medial

19.3 Instability

Shoulder arthroplasty can disturb the complex interplay of bony and soft tissue restraints of the glenohumeral joint. Instability following shoulder arthroplasty is a common complication with a reported prevalence of 4% and accounts for 30% of all complications across multiple studies [8, 12, 29–31]. Specifically, anterior and superior instability accounted for 80% of the cases of instability [8, 12, 29–31]. Superior instability is associated with a deficient rotator cuff or coracoacromial arch [32, 33]. Anterior instability is typically caused by subscapularis insufficiency [5, 30, 34]. Posterior instability is most often caused by residual retroversion of the glenoid component [5, 30, 34].

Plain radiographs can be used to assess prosthesis instability. The axillary radiograph is the gold standard to assess subluxation of the prosthetic head in the sagittal plane. Furthermore, the degree of subluxation can be classified as either absent, slight, moderate, or severe based on the direction and severity (Table 19.2) [35]. Joint widening on the true AP views may also indicate instability, possibly due to an undersized humeral component, an excessive osteotomy, or a deficient rotator cuff [26].

Failure of the subscapularis tendon is implicated in many cases of anterior instability following TSA [36–38], but clear visualization is difficult due to metal artifact. Ultrasound can be extremely accurate in the detection of rotator cuff tears in the postoperative shoulder (Fig. 19.4) [39, 40]. In a study documenting the subscapularis healing rate by the use of postoperative ultrasound after TSA in 30 patients, ultrasound identified four torn tendons, whereas there were no radiographic findings definitively associated with the absence of intact subscapularis tendons [41]. A study by Sofka et al. of 11 shoulder arthroplasty revealed six subscapularis tears [42].

Posterior instability is normally a result of excessive component retroversion [5, 30, 34]. Consequently, posterior glenoid erosion and soft tissue imbalance lead to instability [8]. Posterior subluxation can be seen on the axillary radiograph (Fig. 19.5). A CT can also be used to determine glenoid version accurately [39].

19.4 Periprosthetic Fracture

The reported prevalence of periprosthetic humeral fractures has been estimated to be between 1.5% and 3% [30, 43]. Initial evaluation of a suspected fracture in a patient should include AP and axillary radiographs. Cofield and Wright developed a classification system for humeral periprosthetic fractures [44]. Type A fractures occur at the tip of the prosthesis and extend proximally. Type B fractures occur at the tip of the prosthesis without extension. Type C fractures occur at the prosthetic tip and have distal extension [44].

Fig. 19.5 Axillary radiograph showing posterior subluxation of the humeral head component secondary to eccentric posterior glenoid wear

19.5 Rotator Cuff Tear

19.5.1 Case 2

A 73-year-old right-hand-dominant male who originally underwent a right total shoulder replacement at an outside hospital approximately 18 months prior to presentation with pain and limited function. Physical exam revealed pseudoparalysis with attempted elevation and anterosuperior escape. Radiographs show superior and anterior subluxation (Fig. 19.6a, b), and MRI showed subscapularis dehiscence with retraction to the coracoid (Fig. 19.7) and fatty infiltration of the muscle belly.

Patient underwent conversion of his total shoulder replacement to a reverse shoulder arthroplasty (Fig. 19.8). Four years later, the patient now has 150° of forward flexion, 15° of external rotation, and internal rotation to the back pocket all with minimal pain.

Rotator cuff tears can be assessed radiographically by observing superior migration of the humeral head and mea-

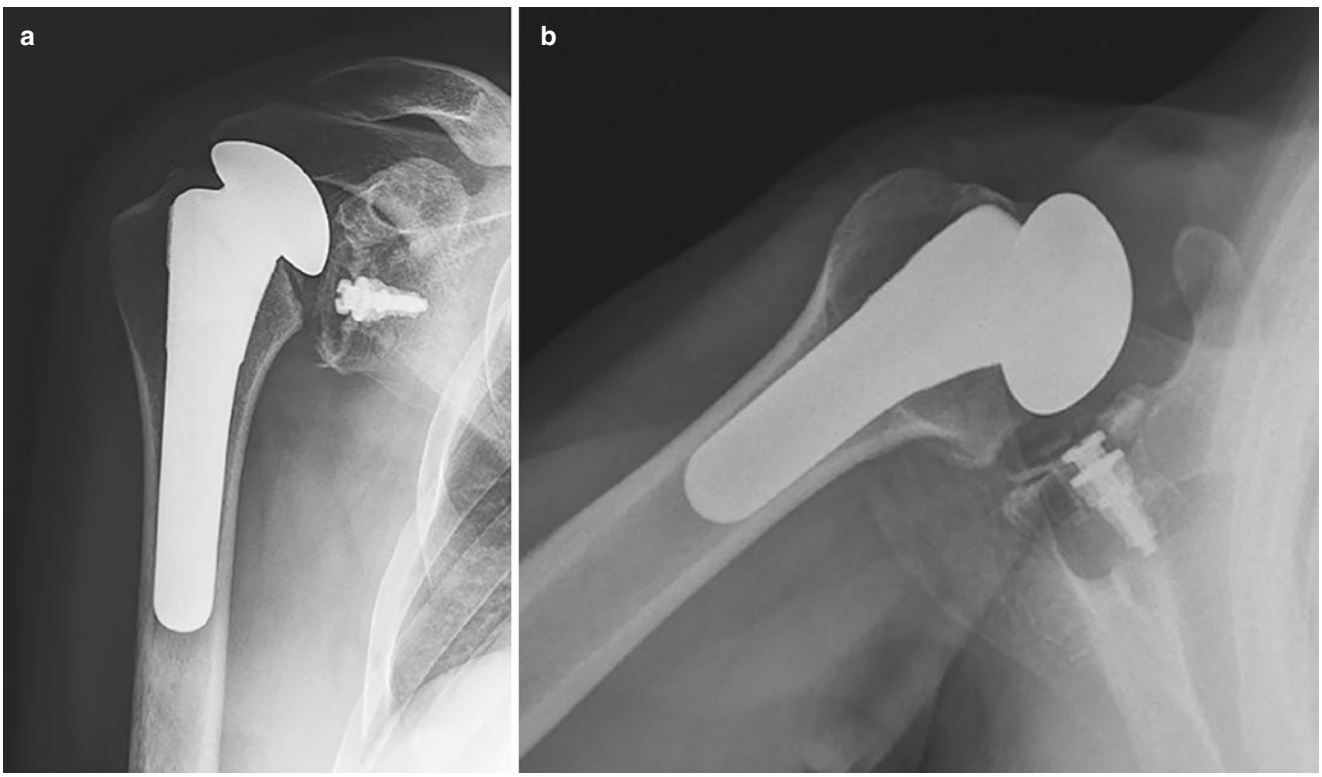

Fig. 19.6 AP (**a**) radiograph shows superior migration of the humeral head, and the axillary (**b**) shows anterior subluxation. Both indicative of a rotator cuff tear

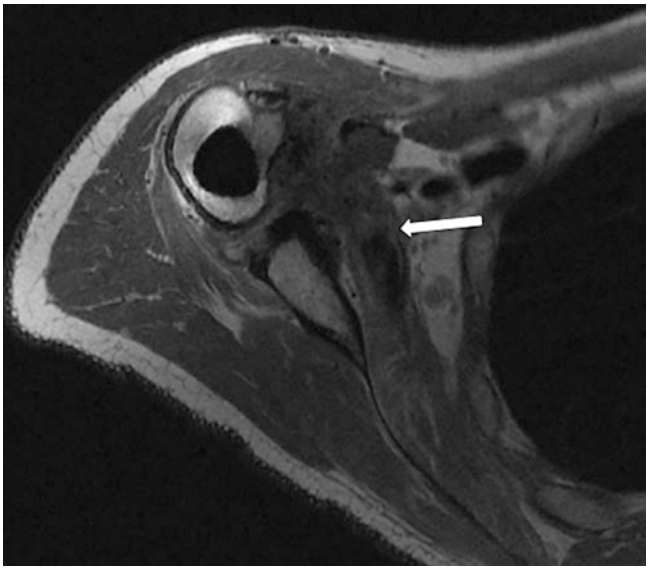

Fig. 19.7 MRI showing dehiscence of the subscapularis with retraction of the main tendon stump past the coracoid (*arrow*)

Fig. 19.8 AP radiograph after conversion of the total shoulder replacement to a reverse shoulder arthroplasty

suring a reduction of the acromiohumeral distance. However, this measurement can be imprecise because it varies according to the projection, size, and sex of the patient. Instead, Skirving [15] advocated the importance of the continuity of the scapulohumeral line (analogous to Shenton's line in the hip) on a true AP of the shoulder taken with the arm in neutral or external rotation. When there is a break in this line, it is a more sensitive indicator of superior migration of the humeral head and, therefore, of rotator cuff tears. Despite these findings, plain radiographs have limited ability to assess the integrity of the cuff, the quality of the muscle, and the degree of retraction of a torn tendon.

Consequently, MRI has been relied upon to provide a more accurate diagnosis in the face of clinical and conventional imaging limitations [45]. MRI, however, presents its own particular set of imaging challenges in shoulder arthroplasty due to the magnetic susceptibility generated by the implant resulting in local field distortions that obscure the regional structures. The intensity of the susceptibility artifact is a function of the relative ferromagnetism of the components, with titanium being less ferromagnetic (and thus causing less artifact) than cobalt-chrome alloy components, as well as the orientation of the components relative to the external magnetic field. Additionally, the eccentric location of the shoulder relative to the isocenter of the imaging bore and the large spherical component increase the susceptibility artifact of shoulder arthroplasty when compared to knee or hip arthroplasty [45, 46].

Modifications in conventional fast spin echo techniques have improved visualization of the soft tissues around implants. In an MRI study of 42 painful shoulder arthroplasties, Sperling et al. [45] suggested that MR imaging is a useful tool to determine the integrity of the rotator cuff; however, they found that the lesser tuberosity and glenoid component were obscured by artifact created by the proximal spherical humeral component. Relatively new commercially available pulse sequences, multiacquisition variable-resonance image combination (MAVRIC) and slice-encoding metal artifact correction (SEMAC), can further reduce susceptibility artifact near implants [47–49]. These new pulse sequences rely on conventional imaging techniques and can be used with standard clinical 1.5-T and 3-T MRI hardware.

Early studies have shown that MAVRIC images can detect pathology not visible with standard metal artifact-reduction FSE sequences. Hayter et al. [47] evaluated the quality of MAVRIC images compared with that of metal artifact-reduction FSE images of 27 patients who underwent shoulder arthroplasty. Their findings included significantly improved visualization of the synovium, periprosthetic bone, glenoid osteolysis, and supraspinatus tendon. Importantly, detection of supraspinatus tears was significantly increased with MAVRIC compared with FSE imaging alone (Fig. 19.9a, b). Although the lesser tuberosity and subscapularis footprint often remain obscured, the muscle tendon junction and its muscle belly are typically visualized and should be carefully evaluated for failure, as this is a common cause of anterior instability. Application of MAVRIC or SEMAC to axial images could potentially better elucidate subscapularis tears at the footprint (Fig. 19.7).

By decreasing image distortion and improving visualization of the bone-prosthesis interface, these new metal

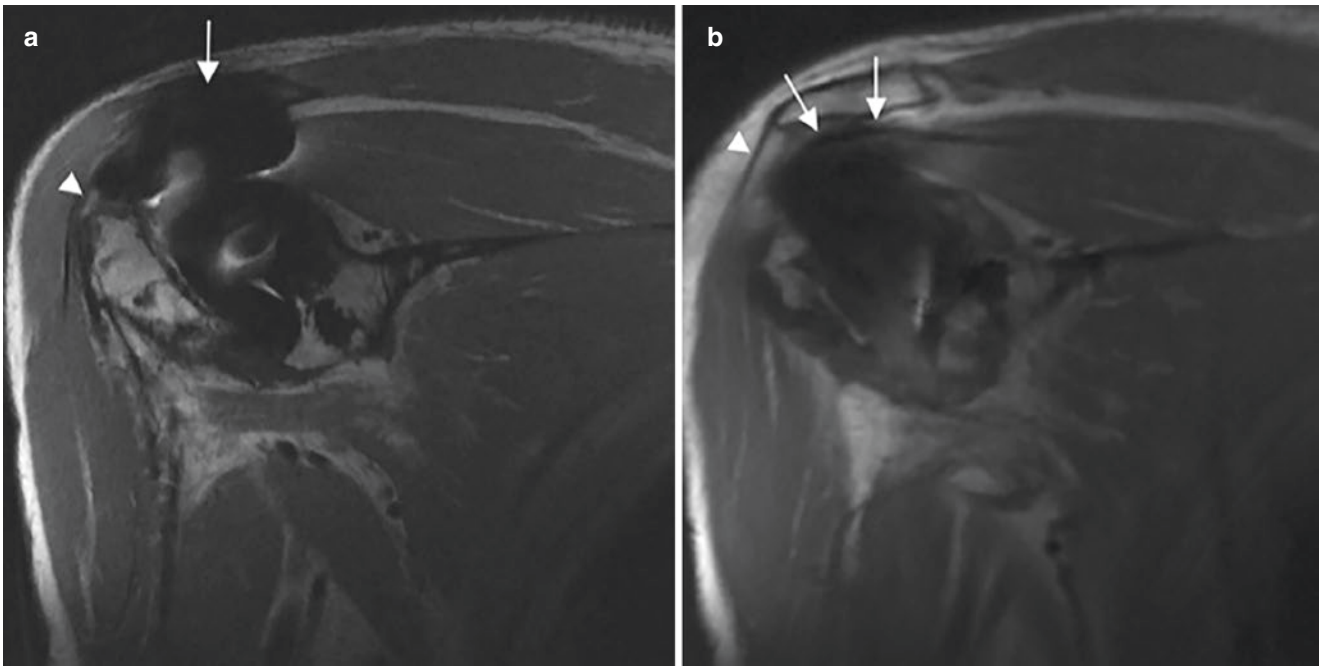

Fig. 19.9 (**a**) Coronal oblique FSE proton density image demonstrates bulky dephasing artifact superiorly obstructing the supraspinatus muscle tendon junction (*arrow*). Note that the supraspinatus footprint (*arrowhead*) remains visualized, which is hyperintense in this case indicating tendinosis but no tear. (**b**) Coronal oblique MAVRIC FSE proton density image allows visualization of the supraspinatus muscle tendon junction (*arrows*), thereby increasing the ability to detect supraspinatus tendon tears and retraction. Note the ability to see the origin of the deltoid (*arrowhead*)

reduction techniques (MAVRIC/SEMAC) serve to complement conventional FSE images, which ultimately offer higher spatial resolution than MAVRIC images, thus providing greater detail of the visualized soft tissues [47].

Similar to MRI, ultrasound is able to assess periarticular soft tissues without radiation; however, sonography has the added benefits of eliminating interference from the implant and allowing dynamic examinations. Westhoff et al. [50] performed static and dynamic ultrasound examinations on 22 patients, and results were correlated with clinical outcome. Pathologic changes within the supraspinatus and infraspinatus tendons were found in several shoulders. A halo sign around the biceps tendon was detected in seven shoulders (Fig. 19.10). This low-echogenic halo around the biceps tendon correlated well with fluid in the synovial sheath and indicated effusion within the glenohumeral joint according to a study by Rupp et al. [51]. Increased intra-articular volume was detected in five patients, two of whom also had a halo sign around the biceps tendon. Subdeltoid bursitis was found in only one shoulder. Loosening of the glenoid during dynamic examination was detected in one shoulder. Pathological findings also correlated well with poorer outcomes, while lack of findings correlated with better outcomes.

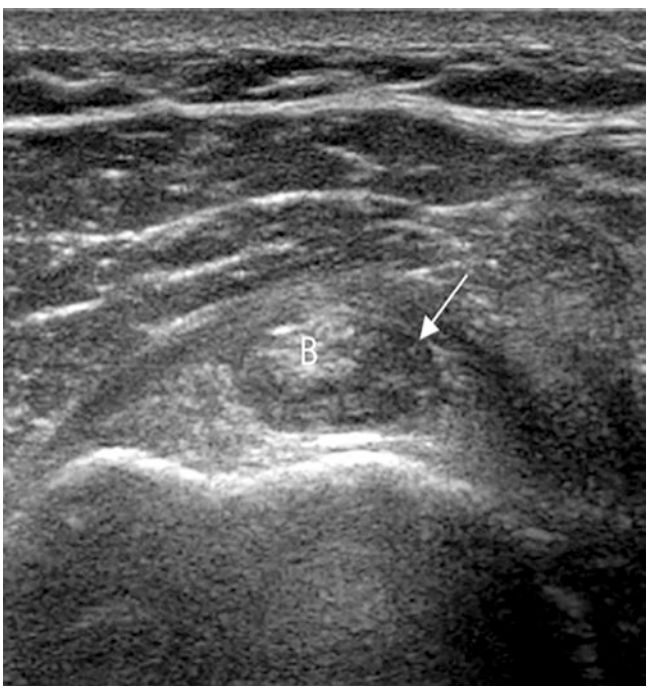

Fig. 19.10 Ultrasound image demonstrates the long head of the biceps tendon (B) in short axis with a hypoechoic rim of synovial fluid and debris (*arrow*)—"halo" sign

Sofka and Adler [42] performed ultrasound examinations on 11 shoulder arthroplasty patients who had clinical suspicion of rotator cuff tear, pain, and decreased range of motion. Sonographic findings included six supraspinatus tendon tears and three infraspinatus tendon tears. Nine patients had biceps tendinosis. The prosthesis did not hinder examination of the rotator cuff in any patient (Fig. 19.11). The authors concluded that sonography is a rapid and reliable method to use for evaluating the periprosthetic soft tissues, including the rotator cuff, in patients who have undergone shoulder replacement. Disadvantages of ultrasound are that it does not give a global picture of the joint and it provides limited evaluation of component loosening [52].

Despite the relatively common use of MRI and ultrasound for evaluation of most soft tissue shoulder abnormalities, CT arthrography can also provide an accurate assessment of the rotator cuff, the capsular-labral-ligamentous structures, and the articular cartilage of the glenohumeral joint [53, 54]. Multi-detector CT (MDCT) is a development that has provided excellent spatial resolution and multiplanar capability, thus markedly improving the diagnostic power of CT arthrography of the shoulder [55]. Some authors [56, 57] prefer MDCT arthrography for imaging patients with shoulder prostheses because the images have minimal artifacts while allowing sufficient assessment of prosthetic and periprosthetic bony and soft tissue abnormalities. Post-processing of volume-rendered 3D CT can also substantially reduce beam-hardening artifacts and can be used to assess hardware integrity [58]. Additionally, joint fluid can be aspirated during the intra-articular administration of contrast medium and sent for culture and sensitivity testing if clinical suspicion of infection warrants [59]. General indications for MDCT arthrography pertain to the inability to perform MRI or failure of MRI to adequately evaluate the shoulder. For example, indications include the presence of metal hardware close to the joint, the presence of MRI-incompatible implanted medical devices, and a history of claustrophobia. In patients who have undergone shoulder surgery, MDCT arthrography has been found to be more accurate than nonarthrographic MRI [60]. However, to date, there has not been a direct comparison of MDCT arthrography and MR arthrography.

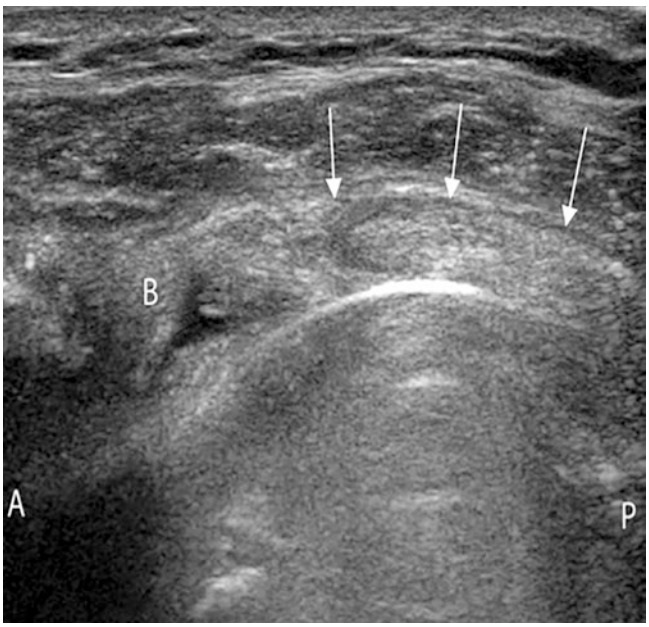

Fig. 19.11 Short axis ultrasound image shows an intact supraspinatus tendon (*arrows*). The hyperechoic curvilinear line deep to the supraspinatus is the humeral component. *B* biceps long head tendon

19.6 Infection

Although infection is a rare complication of primary shoulder arthroplasty, it can have devastating consequences. Bohsali [8] found an overall prevalence of 0.7% across several studies. Susceptible host-related factors for infection include diabetes, rheumatoid arthritis, systemic lupus erythematosus, previous surgery, and remote sources of infection. Extrinsic causes of infection include chemotherapy, systemic corticosteroid therapy, and repeated intra-articular steroid injections [5, 30].

Clinically, pain is usually the most common symptom. Laboratory tests such as measurements of the C-reactive protein level, erythrocyte sedimentation rate, and white blood cell count are important indicators of infection [5, 30]. The two most common organisms responsible for infections after shoulder surgery are *Propionibacterium acnes and Staphylococci*, which are mainly coagulase negative [61]. A well-fixed humeral component that later becomes loose is considered to be infected until proven otherwise [62].

On plain radiographs, there are some nonspecific findings that are suggestive of infection. These include periosteal reaction, scattered foci of osteolysis, or generalized bone resorption in the absence of implant wear [61]. In fact, in the early stages of infection, plain radiographs may be normal in appearance. Radiographs, however, can be extremely helpful in ruling out other conditions such as dislocation and periprosthetic fractures [63].

The current imaging modality of choice for evaluation of suspected joint replacement infection is radionuclide imaging because it is generally not affected by metallic hardware [64]. Advantages of bone scintigraphy are that it is widely available, relatively inexpensive, and easily performed [65]. In a study of 72 total joint replacements, Levitsky and colleagues [66] showed that bone scintigraphy had a sensitivity of 33%, a specificity of 86%, a positive predictive value of 30%, and a negative predictive value of 88%. A standard protocol of combined radionuclide imaging has been established to improve specificity. The technetium scan is performed first to reveal all areas of high metabolic activity. Next,

indium-111, which targets leukocytes, accumulates in regions of inflammation. Superimposing these results can help distinguish true infection from uninflamed areas of high metabolic activity such as fracture or remodeling [61]. F-fluorodeoxyglucose positron emission tomography (FDG-PET) appears to have numerous advantages over conventional radionuclide imaging such as improved spatial resolution within a short time [67]. Unfortunately, data on FDG-PET suggest there is no additional benefit over conventional nuclear medicine modalities in diagnosing prosthetic joint infections [68–70]. Therefore, radionuclide imaging should be used as an adjunct to support a diagnosis of infection when serologic findings are abnormal or equivocal [61].

19.7 Conclusion

While shoulder arthroplasty is extremely successful in the majority of patients, its estimated 15% complication rate should raise the examining clinician's suspicion when pain is the chief complaint. Common complications include component loosening, instability, periprosthetic fracture, rotator cuff tear, and infection. Correct diagnosis and ultimately improved patient care depend on a careful history and physical combined with the selection of the imaging modality that will best highlight the pathological change suspected.

References

1. Barrett WP, Thornhill TS, Thomas WH, Gebhart EM, Sledge CB. Nonconstrained total shoulder arthroplasty in patients with polyarticular rheumatoid arthritis. J Arthroplast. 1989;4(1):91–6. https://doi.org/10.1016/S0883-5403(89)80058-0.
2. Barrett W, Franklin J, Jackins S, Wyss C, Matsen F. Total shoulder arthroplasty. J Bone Jt Surg Am. 1987;69(6):865–72.
3. Cofield RH. Total shoulder arthroplasty with the Neer prosthesis. J Bone Joint Surg Am. 1984;66(6):899–906. https://doi.org/10.2106/00004623-198466060-00010.
4. Cofield RH, Edgerton BC. Total shoulder arthroplasty: complications and revision surgery. Instr Course Lect. 1990;39:449–62.
5. Matsen FA III, Rockwood CA, Wirth MA, Lippitt SB. Glenohumeral arthritis and its management. In: Rockwood Jr C, Matsen III F, editors. The shoulder, vol. 2. Elsevier Health Sciences; 2009. p. 840–964.
6. Hasan SS, Leith JM, Campbell B, Kapil R, Smith KL, Matsen FA. Characteristics of unsatisfactory shoulder arthroplasties. J Shoulder Elb Surg. 2002;11(5):431–41. https://doi.org/10.1067/MSE.2002.125806.
7. Brenner BC, Ferlic DC, Clayton ML, Dennis DA. Survivorship of unconstrained total shoulder arthroplasty. J Bone Jt Surg Am. 1989;71(9):1289–96.
8. Bohsali KI, Wirth MA, Rockwood CA Jr. Complications of total shoulder arthroplasty. J Bone Jt Surg Am. 2006;88(10):2279–92.
9. Norris TR. Fracture and fracture dislocations of the glenohumeral complex. In: Chapman MW, Madison M, editors. Operative Orthopaedics. Lippincott Williams & Wilkins; 1993. p. 405–24.
10. Iannotti JP, Gabriel JP, Schneck SL, Evans BG, Misra S. The normal glenohumeral relationships. An anatomical study of one hundred and forty shoulders. J Bone Jt Surg Am. 1992;74(4):491–500.
11. Figgie HE, Inglis AE, Goldberg VM, Ranawat CS, Figgie MP, Wile JM. An analysis of factors affecting the long-term results of total shoulder arthroplasty in inflammatory arthritis. J Arthroplast. 1988;3(2):123–30.
12. Deshmukh AV, Koris M, Zurakowski D, Thornhill TS. Total shoulder arthroplasty: long-term survivorship, functional outcome, and quality of life. J Shoulder Elb Surg. 2005;14(5):471–9. https://doi.org/10.1016/J.JSE.2005.02.009.
13. Franklin JL, Barrett WP, Jackins SE, Matsen FA. Glenoid loosening in total shoulder arthroplasty. Association with rotator cuff deficiency. J Arthroplast. 1988;3(1):39–46. https://doi.org/10.1016/S0883-5403(88)80051-2.
14. Lazarus MD, Jensen KL, Southworth C, Matsen FA. The radiographic evaluation of keeled and pegged glenoid component insertion. J Bone Joint Surg Am. 2002;84(7):1174–82. https://doi.org/10.2106/00004623-200207000-00013.
15. Skirving AP. Total shoulder arthroplasty -- current problems and possible solutions. J Orthop Sci. 1999;4(1):42–53. https://doi.org/10.1007/S007760050073.
16. Boileau P, Watkinson DJ, Hatzidakis AM, Balg F. Grammont reverse prosthesis: design, rationale, and biomechanics. J Shoulder Elb Surg. 2005;14(1 Suppl S):S147–61. https://doi.org/10.1016/J.JSE.2004.10.006.
17. Werner CML, Steinmann PA, Gilbart M, Gerber C. Treatment of painful pseudoparesis due to irreparable rotator cuff dysfunction with the Delta III reverse-ball-and-socket total shoulder prosthesis. J Bone Joint Surg Am. 2005;87(7):1476–86. https://doi.org/10.2106/JBJS.D.02342.
18. Sirveaux F, Favard L, Oudet D, Huquet D, Walch G, Molé D. Grammont inverted total shoulder arthroplasty in the treatment of glenohumeral osteoarthritis with massive rupture of the cuff. Results of a multicentre study of 80 shoulders. J Bone Joint Surg Br. 2004;86(3):388–95. https://doi.org/10.1302/0301-620X.86B3.14024.
19. Grassi FA, Murena L, Valli F, Alberio R. Six-year experience with the Delta III reverse shoulder prosthesis. J Orthop Surg (Hong Kong). 2009;17(2):151–6. https://doi.org/10.1177/230949900901700205.
20. John M, Pap G, Angst F, et al. Short-term results after reversed shoulder arthroplasty (Delta III) in patients with rheumatoid arthritis and irreparable rotator cuff tear. Int Orthop. 2010;34(1):71. https://doi.org/10.1007/S00264-009-0733-1.
21. Lévigne C, Garret J, Boileau P, Alami G, Favard L, Walch G. Scapular notching in reverse shoulder arthroplasty: is it important to avoid it and how? Clin Orthop Relat Res. 2011;469(9):2512–20. https://doi.org/10.1007/S11999-010-1695-8.
22. Nyffeler RW, Werner CML, Gerber C. Biomechanical relevance of glenoid component positioning in the reverse Delta III total shoulder prosthesis. J Shoulder Elb Surg. 2005;14(5):524–8. https://doi.org/10.1016/J.JSE.2004.09.010.
23. Levy JC, Virani N, Pupello D, Frankle M. Use of the reverse shoulder prosthesis for the treatment of failed hemiarthroplasty in patients with glenohumeral arthritis and rotator cuff deficiency. J Bone Joint Surg Br. 2007;89(2):189–95. https://doi.org/10.1302/0301-620X.89B2.18161.
24. Cuff D, Pupello D, Virani N, Levy J, Frankle M. Reverse shoulder arthroplasty for the treatment of rotator cuff deficiency. J Bone Jt Surg - Ser A Published online. 2008; https://doi.org/10.2106/JBJS.G.00775.
25. Kalouche I, Sevivas N, Wahegaonker A, Sauzieres P, Katz D, Valenti P. Reverse shoulder arthroplasty: does reduced medialisation improve radiological and clinical results? Acta Orthop Belg. 2009;75(2):158–66.

26. Merolla G, Di Pietto F, Romano S, Paladini P, Campi F, Porcellini G. Radiographic analysis of shoulder anatomical arthroplasty. Eur J Radiol. 2008;68(1):159–69. https://doi.org/10.1016/J.EJRAD.2008.07.021.
27. Sanchez-Sotelo J, Wright TW, O'Driscoll SW, Cofield RH, Rowland CM. Radiographic assessment of uncemented humeral components in total shoulder arthroplasty. J Arthroplast. 2001;16(2):180–7. https://doi.org/10.1054/ARTH.2001.20905.
28. Sperling JW, Cofield RH, O'Driscoll SW, Torchia ME, Rowland CM. Radiographic assessment of ingrowth total shoulder arthroplasty. J Shoulder Elb Surg. 2000;9(6):507–13. https://doi.org/10.1067/MSE.2000.109384.
29. Stewart MPM, Kelly IG. Total shoulder replacement in rheumatoid disease: 7- to 13-year follow-up of 37 joints. J Bone Joint Surg Br. 1997;79(1):68–72. https://doi.org/10.1302/0301-620X.79B1.6645.
30. Wirth MA, Rockwood CA. Complications of total shoulder-replacement arthroplasty. J Bone Joint Surg Am. 1996;78(4):603–16. https://doi.org/10.2106/00004623-199604000-00018.
31. Sperling JW, Cofield RH, Rowland CM. Neer hemiarthroplasty and Neer total shoulder arthroplasty in patients fifty years old or less. Long-term results. J Bone Joint Surg Am. 1998;80(4):464–73. https://doi.org/10.2106/00004623-199804000-00002.
32. Neer CS. Replacement arthroplasty for glenohumeral osteoarthritis. J Bone Jt Surg Am. 1974;56(1):1–13.
33. Jahnke AH, Hawkins RJ. Instability after shoulder arthroplasty: causative factors and treatment options. Semin Arthroplast. 1995;6(4):289–96.
34. Brems JJ. Complications of shoulder arthroplasty: infections, instability, and loosening. Instr Course Lect. 2002;51:29–39.
35. Sperling JW, Cofield RH, Rowland CM. Minimum fifteen-year follow-up of Neer hemiarthroplasty and total shoulder arthroplasty in patients aged fifty years or younger. J Shoulder Elb Surg. 2004;13(6):604–13. https://doi.org/10.1016/S1058274604001296.
36. Gartsman GM, Russell JA, Gaenslen E. Modular shoulder arthroplasty. J Shoulder Elb Surg. 1997;6(4):333–9. https://doi.org/10.1016/S1058-2746(97)90000-8.
37. Hawkins RJ, Bell RH, Jallay B. Total shoulder arthroplasty. Clin Orthop Relat Res. 1989;242:188–94.
38. Middleton WD, Reinus WR, Totty WG, Melson CL, Murphy WA. Ultrasonographic evaluation of the rotator cuff and biceps tendon. J Bone Jt Surg Am. 1986;68(3):440–50.
39. Hennigan SP, Iannotti JP. Instability after prosthetic arthroplasty of the shoulder. Orthop Clin North Am. 2001;32(4):649–59. https://doi.org/10.1016/S0030-5898(05)70234-0.
40. Stefko JM, Jobe FW, VanderWilde RS, Carden E, Pink M. Electromyographic and nerve block analysis of the subscapularis liftoff test. J Shoulder Elb Surg. 1997;6(4):347–55. https://doi.org/10.1016/S1058-2746(97)90002-1.
41. Armstrong A, Lashgari C, Teefey S, Menendez J, Yamaguchi K, Galatz LM. Ultrasound evaluation and clinical correlation of subscapularis repair after total shoulder arthroplasty. J Shoulder Elb Surg. 2006;15(5):541–8. https://doi.org/10.1016/J.JSE.2005.09.013.
42. Sofka CM, Adler RS. Original report. Sonographic evaluation of shoulder arthroplasty. AJR Am J Roentgenol. 2003;180(4):1117–20. https://doi.org/10.2214/AJR.180.4.1801117.
43. Kumar S, Sperling JW, Haidukewych GH, Cofield RH. Periprosthetic humeral fractures after shoulder arthroplasty. J Bone Joint Surg Am. 2004;86(4):680–9. https://doi.org/10.2106/00004623-200404000-00003.
44. Wright TW, Cofield RH. Humeral fractures after shoulder arthroplasty. J Bone Joint Surg Am. 1995;77(9):1340–6. https://doi.org/10.2106/00004623-199509000-00008.
45. Sperling JW, Potter HG, Craig EV, Flatow E, Warren RF. Magnetic resonance imaging of painful shoulder arthroplasty. J Shoulder Elb Surg. 2002;11(4):315–21. https://doi.org/10.1067/MSE.2002.124426.
46. Potter HG, Foo LF. Magnetic resonance imaging of joint arthroplasty. Orthop Clin North Am. 2006;37(3):361–73. https://doi.org/10.1016/J.OCL.2006.03.003.
47. Hayter CL, Koff MF, Shah P, Koch KM, Miller TT, Potter HG. MRI after arthroplasty: comparison of MAVRIC and conventional fast spin-echo techniques. AJR Am J Roentgenol. 2011;197(3) https://doi.org/10.2214/AJR.11.6659.
48. Koch KM, Lorbiecki JE, Hinks RS, King KF. A multispectral three-dimensional acquisition technique for imaging near metal implants. Magn Reson Med. 2009;61(2):381–90. https://doi.org/10.1002/MRM.21856.
49. Koch KM, Brau AC, Chen W, et al. Imaging near metal with a MAVRIC-SEMAC hybrid. Magn Reson Med. 2011;65(1):71–82. https://doi.org/10.1002/MRM.22523.
50. Westhoff B, Wild A, Werner A, Schneider T, Kahl V, Krauspe R. The value of ultrasound after shoulder arthroplasty. Skelet Radiol. 2002;31(12):695–701. https://doi.org/10.1007/S00256-002-0555-3.
51. Rupp S, Seil R, Kohn D. Significance of the hypoechoic area around the long biceps tendon in shoulder sonography--underlying pathology. Z Orthop Ihre Grenzgeb. 1999;137(1):7–9. https://doi.org/10.1055/S-2008-1037028.
52. McMenamin D, Koulouris G, Morrison WB. Imaging of the shoulder after surgery. Eur J Radiol. 2008;68(1):106–19. https://doi.org/10.1016/J.EJRAD.2008.02.050.
53. Buckwalter KA. CT arthrography. Clin Sports Med. 2006;25(4):899–915. https://doi.org/10.1016/J.CSM.2006.06.002.
54. De Jesus JO, Parker L, Frangos AJ, Nazarian LN. Accuracy of MRI, MR arthrography, and ultrasound in the diagnosis of rotator cuff tears: a meta-analysis. AJR Am J Roentgenol. 2009;192(6):1701–7. https://doi.org/10.2214/AJR.08.1241.
55. Cody DD. AAPM/RSNA physics tutorial for residents: topics in CT: image processing in CT. Radiographics. 2002;22(5):1255–68. https://doi.org/10.1148/RADIOGRAPHICS.22.5.G02SE041255/ASSET/IMAGES/LARGE/G02SE04C18B.JPEG.
56. Woertler K. Multimodality imaging of the postoperative shoulder. Eur Radiol. 2007;17(12):3038–55. https://doi.org/10.1007/S00330-007-0649-3.
57. Lee MJ, Kim S, Lee SA, et al. Overcoming artifacts from metallic orthopedic implants at high-field-strength MR imaging and multi-detector CT. Radiographics. 2007;27(3):791–803. https://doi.org/10.1148/RG.273065087.
58. Fayad LM, Johnson P, Fishman EK. Multidetector CT of musculoskeletal disease in the pediatric patient: principles, techniques, and clinical applications. Radiographics. 2005;25(3):603–18. https://doi.org/10.1148/RG.253045092.
59. Fritz J, Fishman EK, Small KM, et al. MDCT arthrography of the shoulder with datasets of isotropic resolution: indications, technique, and applications. AJR Am J Roentgenol. 2012;198(3):635–46. https://doi.org/10.2214/AJR.11.7078.
60. De Filippo M, Bertellini A, Sverzellati N, et al. Multidetector computed tomography arthrography of the shoulder: diagnostic accuracy and indications. Acta Radiol. 2008;49(5):540–9. https://doi.org/10.1080/02841850801935559.
61. Bauer TW, Parvizi J, Kobayashi N, Krebs V. Diagnosis of periprosthetic infection. J Bone Joint Surg Am. 2006;88(4):869–82. https://doi.org/10.2106/JBJS.E.01149.
62. Sperling JW, Hawkins RJ, Walch G, Mahoney AP, Zuckerman JD. Complications in total shoulder arthroplasty. Instr Course Lect. 2013;62:135–41.
63. Palestro CJ, Love C, Miller TT. Infection and musculoskeletal conditions: imaging of musculoskeletal infections. Best Pract Res Clin Rheumatol. 2006;20(6):1197–218. https://doi.org/10.1016/J.BERH.2006.08.009.

64. Love C, Marwin SE, Palestro CJ. Nuclear medicine and the infected joint replacement. Semin Nucl Med. 2009;39(1):66–78. https://doi.org/10.1053/J.SEMNUCLMED.2008.08.007.
65. Gemmel F, Van Den Wyngaert H, Love C, Welling MM, Gemmel P, Palestro CJ. Prosthetic joint infections: radionuclide state-of-the-art imaging. Eur J Nucl Med Mol Imaging. 2012;39(5):892–909. https://doi.org/10.1007/S00259-012-2062-7.
66. Levitsky KA, Hozack WJ, Balderston RA, et al. Evaluation of the painful prosthetic joint. Relative value of bone scan, sedimentation rate, and joint aspiration. J Arthroplast. 1991;6(3):237–44. https://doi.org/10.1016/S0883-5403(06)80170-1.
67. De Winter F, Van De Wiele C, Vogelaers D, De Smet K, Verdonk R, Dierckx RA. Fluorine-18 fluorodeoxyglucose-position emission tomography: a highly accurate imaging modality for the diagnosis of chronic musculoskeletal infections. J Bone Joint Surg Am. 2001;83(5) https://doi.org/10.2106/00004623-200105000-00002.
68. Love C, Marwin SE, Tomas MB, et al. Diagnosing infection in the failed joint replacement: a comparison of coincidence detection 18F-FDG and 111In-labeled leukocyte/99mTc-sulfur colloid marrow imaging. J Nucl Med. 2004;45(11):1864–71.
69. Zhuang H, Duarte PS, Pourdehnad M, et al. The promising role of 18F-FDG PET in detecting infected lower limb prosthesis implants. J Nucl Med. 2001;42(1):44–8.
70. Kwee TC, Kwee RM, Alavi A. FDG-PET for diagnosing prosthetic joint infection: systematic review and metaanalysis. Eur J Nucl Med Mol Imaging. 2008;35(11):2122–32. https://doi.org/10.1007/S00259-008-0887-X.